Seismic Design and Application of Hybrid Coupled Walls with Replaceable Steel Coupling Beams in High-Rise Buildings

Xiaodong Ji[1] and Carlos Molina Hutt[2]
[1]*Department of Civil Engineering, Key Laboratory of Civil Engineering Safety and Durability of China Education Ministry, Tsinghua University, Beijing 100084, China*
[2]*Department of Civil Engineering, University of British Columbia, Vancouver, BC, Canada V6Z1Z4*

SUMMARY

An innovative hybrid coupled wall (HCW) system consists of reinforced concrete (RC) wall piers connected with replaceable steel coupling beams (RSCBs) throughout their height. The RSCBs are designed with a central 'fuse' shear link connected to steel beam segments at both ends, which are capacity designed to remain elastic. During a damaging earthquake, the 'fuse' shear links yield and dissipate seismic energy, and once damaged, they can be easily replaced due to specialized link-to-beam connection details. Therefore, this system is expected to provide enhanced seismic performance over conventional RC coupled wall (RCW) system, particularly in terms of repair costs and time after damaging earthquakes. This paper presents an overview of seismic design considerations of this new system, which is intended as a guide for design practitioners to adopt the system. Design procedure of this system is first summarized, followed by description of the coupling ratio selection, member sizing, connection detailing and modelling recommendations of the system. Furthermore, an analytical case study for a high-rise building is presented to highlight the benefit of using this system for enhancement to overall building performance. In the end, this paper presents a few real-world applications of RSCBs in super-tall buildings in China.

KEYWORDS:

Replaceable steel coupling beam (RSCB); Hybrid coupled wall (HCW); Seismic design; Structural detailing; Seismic performance assessment; High-rise buildings; Practical application.

1. INTRODUCTION

Reinforced concrete coupled walls (RCWs) consist of wall piers connected with reinforced concrete (RC) coupling beams throughout their height. RCWs are often used as the structural system for mid and high-rise buildings in areas of moderate to high seismicity because of their recognized strength and stiffness benefits. The coupled wall system provides a lateral stiffness that is significantly greater than that of the wall piers alone. The coupling action induced by the coupling beams leads to the tensile and compressive forces in adjacent wall piers, which can resist a proportion of the overturning moment from lateral loads, thus reducing the bending moment demands that must be resisted by individual walls. Furthermore, the coupling beams enable the dissipation of seismic energy throughout the height of the structure during severe earthquakes, as shown in Figure 1a. The large shear force and deformation demands imposed on coupling beams during an earthquake event have led design practitioners to provide special reinforcement detailing in the coupling beams and their connection into the walls [1]. Due to the complexities associated with such reinforcement details, some engineers and researchers have turned to the use of steel coupling beams instead of RC coupling beams. The resulting structural system is referred to as a hybrid coupled wall (HCW) system [2].

The global mechanics of HCWs are no different from that of RCWs. In response to seismic loads, steel coupling beams in HCWs are designed to dissipate seismic energy in a manner similar to that of link elements in eccentrically braced frames. There is extensive research on the expected behavior and design recommendations of HCWs ([2, 3]) and a number of high-rise buildings have been constructed adopting this system. However, there is growing awareness that even though the system will result in buildings that behave well in terms of life safety, because of significant damage levels, post-earthquake repair can be costly and time consuming, leading to extensive loss of occupancy. As a result, various types of replaceable coupling beams have been proposed and recognized as an alternative to conventional RC or steel coupling beams (e.g. [4], [5], [6], [7] and [8]).

A type of replaceable steel coupling beam (RSCB), which comprises of a central 'fuse' shear link connected to steel beam segments at its two ends, as illustrated in Figure 1c, is discussed in this paper. The concept for RSCBs are as follows. By appropriately proportioning the beam segments and shear link, the inelastic deformation can concentrate in the 'fuse' shear links during severe earthquakes, while the steel beam segments remain elastic, as shown in Figure 1b. Extensive studies (e.g., [9] and [10]) have indicated that a short shear link with proper detailing can provide stable and ductile behavior under cyclic shear loading, enabling significant dissipation of seismic energy. By development and adoption of specialized connections between the links and beam segments, the 'fuse' links can be easily replaced after they are damaged during a severe earthquake event [7]. These replaceable fuses enable the structure to swiftly restore its pre-earthquake condition, thus enhancing the seismic performance and resiliency of high-rise buildings.

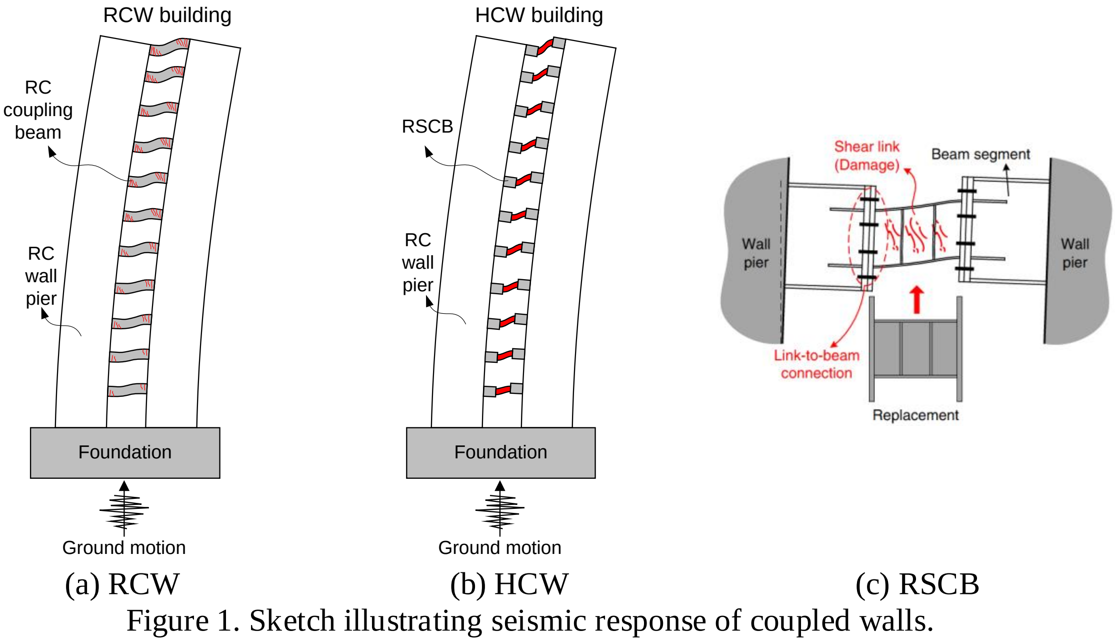

Figure 1. Sketch illustrating seismic response of coupled walls.

With rating systems for resilience-based design gaining momentum (e.g. Resilience-Based Earthquake Design Initiative, United States Resilience Council, etc.), the development of these innovative structural systems is of great relevance. However, in order for design practitioners to adopt such systems, these must be economical, well understood and well documented. This paper is intended as a guide for practicing engineers as it provides an overview of seismic design considerations and performance impacts of adopting the HCW system with RSCBs. The paper is subdivided into four key areas: (i) a review of the system design and member sizing procedure; (ii) recommended connection detailing; (iii) structural analysis modelling recommendations; and (iv) the anticipated performance impact of adopting a HCW system with RSCBs rather than the conventional RCW with RC coupling beams. As illustrated in this paper, through a small number of modifications, which have little impact on the design process, the widely adopted coupled wall structural system can be significantly improved to produce designs of enhanced seismic resilience. The final part of this paper summarizes a few examples of recent applications of the RSCBs in super-tall buildings in China.

2. SYSTEM DESIGN AND MEMBER SIZING

2.1. Design Procedure Overview

At present, modern design codes in the U.S. [11] specify the following design parameters for shear wall systems: a seismic response modification factor, R value, of 5; a displacement amplification factor, C_d, of 5; and a system overstrength factor, Ω_o, of 2.5. If the walls are designed in conjunction with a frame to form a dual system, then R, C_d and Ω_o are 7, 5.5 and 2.5, respectively, and the frame must be designed for at least 25% of the seismic loads and have special detailing.

The recommended prescriptive design procedure outlined by El-Tawil et al. [2, 3] for the design of HCWs with steel coupling beams is also applicable when adopting RSCBs. Figure 2 shows a flowchart for the design procedure of the HCW system. Four major phases are included: (1) preliminary member sizing; (2) structural analysis using linear response spectrum analysis; (3) strength and deformation checks; and (4) detailing structural members and connections. Iterations are required until the design satisfy both strength and displacement limits. Details for the HCW design procedure and considerations can be found in El-Tawil et al. [2, 3]. The following contents highlight a number of key design issues for the HCWs with RSCBs, which might be different from those with conventional steel coupling beams. Note that, the system may be initially proportioned using the performance-based design method, as an alternative to the prescriptive design procedure. Nonlinear response history analysis is recommended in the new-generation performance-based design and assessment method (e.g., FEMA P-58 [12]).

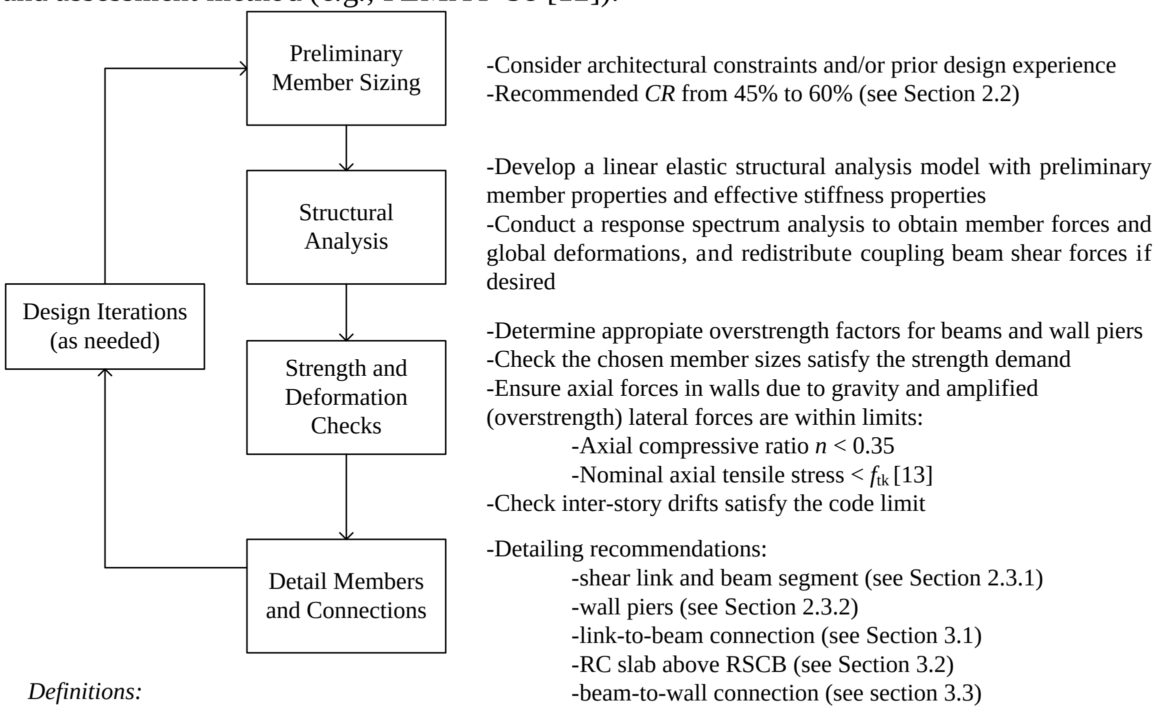

Definitions:
CR is the coupling ratio of the coupled wall system.
$n=N/(f_cA)$ is the axial compressive ratio.
f_{tk} is the nominal tensile strength of concrete.

Figure 2. Design procedure of hybrid coupled wall with RSCBs.

2.2. Coupling Ratio Selection

When a coupled wall is subjected to lateral loads, the overturning moment is resisted by moment reactions developed at the base of the wall piers and coupling action induced by the coupling beams, as shown in Figure 3. Coupling ratio (*CR*) is defined as the proportion of overturning moment resisted by coupling action. Therefore, *CR* is calculated as follows:

$$CR = \frac{TL_{\mathrm{w}}}{TL_{\mathrm{w}} + \sum M_i} \tag{1}$$

where T denotes tensile or compressive force in wall piers induced by shear forces of coupling beams, L_{w} denotes distance between centroids of the adjacent wall piers, and M_i denotes the moment at base of the wall pier. The value of *CR* varies as the coupled wall deforms under lateral loading. Usually, *CR* is calculated at the instance when all the system forms a mechanism, i.e., all coupling beams yield and the wall piers yield at the base. Therefore, the value of *CR* reflects the proportional relation of strengths between the coupling beams and the wall piers.

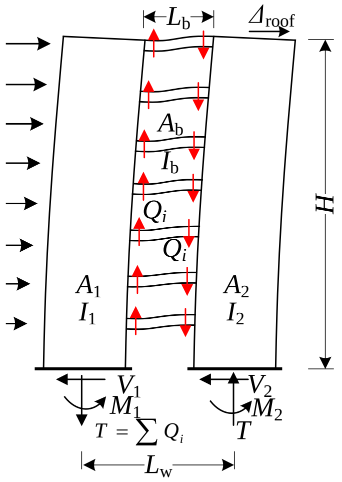

Figure 3. Lateral load resistance pattern of a coupled wall.

A rational amount of *CR* should be considered in the design of a coupled wall system. Small *CR* values lead to wall piers behaving like isolated walls with low overall stiffness, which cannot satisfy the drift limit required by the codes. Large *CR* values lead to excessive tensile and compressive axial forces in wall piers. Large tensile axial forces significantly decrease the stiffness and strength capacity of RC walls [14], while excessive compressive forces significantly decrease the ductility of RC walls. While no requirements are specified to limit *CR* values in the current design codes, i.e. ACI 318 [1], reasonable ranges of *CR* for design can be found in the literature. Harries [15] proposed a practical upper limit of 66% for the *CR* of the hybrid coupled wall system with steel coupling beams. El-Tawil et al. [16] recommend that the *CR* ranges from 30% to 45% for an efficient design of hybrid coupled walls. Liu [17] recommends that the *CR* ranges from 45% to 60% for design of the HCW system with RSCBs for buildings of approximately ten stories in height. The recommendation is obtained from a large amount of nonlinear dynamic analyses of various HCW system with RSCBs subjected to a set of ground motions.

The design philosophy in a HCW system with RSCBs is that the coupling beams will yield first throughout the height of the structure. Energy dissipation in the coupling beams is intended to reduce damage and large displacements of wall pier hinging, which should only be intended to occur under extreme events exceeding the design level earthquake shaking, and only after all coupling beams have yielded. The benefit of adopting a system with RSCBs is limited if the wall piers suffer extensive damage, resulting in excessive residual drifts which compromise the ability of the shear fuse link replacement and overall reparability of the system.

2.3. Member Sizing

2.3.1 Shear Link and Beam Segment

The shear links in RSCBs are generally a rolled or built-up wide flange beam section. Figure 4 shows the typical hysteretic responses of shear links of various length ratios, and summarizes the inelastic rotation collected from tests on 114 shear links. Links that yield in shear provide a more stable and ductile response than those that yield in flexure or flexural-shear mode. The yielding mode is related to the link length ratio $e/(M_p/V_p)$, where e denotes the link length, and M_p and V_p denote the plastic flexural strength and shear strength of the link, respectively. Per AISC 341 [18], properly detailed links with a length ratio smaller than 1.6 are expected to yield primarily in shear and they can reach an inelastic rotation capacity exceeding 0.08 rad. Therefore, a length ratio less than 1.6 is recommended for shear links in RSCBs. In real practice, the short span of coupling beams and the necessity to limit the fuse weight for replacement can lead to the use of very short shear links. Recent tests indicate that very short shear links, with a length ratio less than 1.0, can develop significantly large plastic rotations, reaching approximately 0.14 rad on average [9]. Besides, a hybrid section is recommended for use in built-up links, where the web adopts a lower strength grade steel to decrease the web compactness ratio, and the flanges adopt a higher strength grade steel to provide sufficient moment capacity. The use of a low-yield-strength steel web can lead to a further increase of the maximum inelastic rotation and cumulative plastic rotation capacity of the shear links.

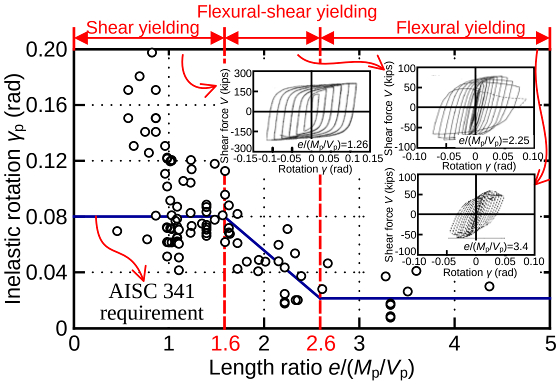

Figure 4. Length ratio versus inelastic rotation capacity of shear links.

The plastic shear strength of the shear link is calculated as V_p=0.6$f_y A_w$, where f_y denotes the steel yield strength of the link web, and A_w denotes the cross sectional area of the link web. V_n, defined as the inelastic strength of the link, is calculated as the smaller of V_p or 2M_p/e. In reality, the maximum shear strength V_{max} of a shear link is larger than its plastic shear strength V_p, due to hardening effect after yielding. Figure 5 summarizes overstrength data, V_{max}/V_n, from steel link tests of various length ratios. The overstrength factor of 1.5, as suggested in AISC 341 [18], is somewhat conservative for shear links with a length ratio of over 1.0. However, the shear links with a length ratio smaller than 1.0 can develop overstrength factors significantly larger than 1.5, ranging from 1.7 to 2.0. An overstrength factor of 1.9 is recommended for links with a length ratio less than 1.0. The large overstrength for very short shear links is resulted from two causes: (1) shear contribution of flanges, and (2) the cyclic hardening effect of web steel under large inelastic strains. The sophisticated finite element analysis in Reference [9] indicates that the contribution of both causes increases along with decrease of the link length ratio and corresponding increase of link inelastic rotation. Note that, the link overstrength is also related to the strength grade of the web steel, as low-yield-strength steel exhibits higher hardening effects. The overstrength data summarized in Figure 5 corresponds to the web steel with a yield strength of no less than 225 MPa. Tests by Dusicka et al [19] indicate that steel links with LY 100 (f_y = 100 MPa) web steel can generate a very large overstrength of approximately 4.9. If LY 100 steel is used in the web of the shear links, special attention should be given to the overstrength parameters adopted.

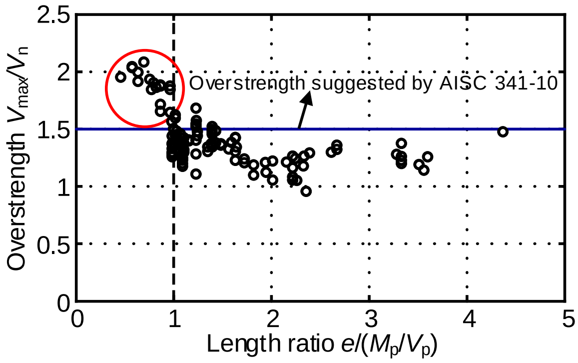

Figure 5. Length ratio versus inelastic rotation capacity of shear links [9].

In order to prevent premature buckling and welding fracture and to ensure sufficient inelastic deformation capacity in the links of RSCBs, the detailing requirements outlined in AISC 341 [18] for links in eccentrically braced frames (EBFs) can be followed, including width-to-thickness ratios of flanges and web, stiffener arrangement and welding requirements.

To ensure that the beam segments remain elastic when the shear link fully yields, their flexural and shear strength should be designed to exceed the strength demand corresponding to the overstrength of shear links. In the calculation, a reasonable overstrength factor shall be determined according to the link length ratio and web steel types. As described previously, the value of overstrength factor for normal-strength steel links is recommended as 1.5 for the links with a length ratio over 1.0, and as 1.9 for the links with a length ratio less than 1.0.

2.3.2 Wall Piers

To ensure that the coupling beams yield prior to the wall piers, it is necessary to design the walls to be stronger that the coupling beams. This is achieved by applying an overstrength factor to the wall design forces. Per AISC 341 [18], the required overstrength is taken as the ratio of the sum of the nominal shear capacities of the coupling beams times $1.1R_y$, to account for expected material strength and strain hardening effects, to the sum of the coupling beam shear design forces as calculated under design load combinations. Note that R_y factor accounts for material overstrength, which is defined as the ratio of the expected yield stress of steel to the specified minimum yield stress.

Even though choosing a high CR for the design of the system will reduce the wall design shear forces and bending moments, required wall overstrengths can result in considerable amplification of the design forces. This effect can be minimized by allowing for redistribution of beam design forces, which can enable a more efficient design. For instance, the Canadian Standards Association [20] permits up to 20% redistribution of shear forces between beams as long as the sum of the beam shear capacities exceeds the sum of the factored beam shears. This not only reduces wall design forces, but also facilitates constructability as it enables the use of the same RSCBs across multiple levels.

In order to ensure sufficient inelastic deformation capacity in the wall piers, the detailing requirements outlined in ACI 318 [1] should be followed, including the distributed reinforcement ratio, limit to shear stress, limit to axial force ratio, and details of the boundary elements.

3. CONNECTION DETAILING

3.1. Link-to-beam Connection

Based on extensive experimental testing [7], two types of beam-to-link connections are recommended: (i) end plate connection, and (ii) splice plate connection. Figures 6 and 7 illustrate a schematic of the proposed connection details. To ensure easy replacement of damaged links, these connections must be capacity designed to exceed the overstrength of the shear link as follows:

$$V_c \geq \Omega V_n \tag{2a}$$

$$M_c \geq 0.5e' \left(\Omega V_n\right) \tag{2b}$$

where V_c and M_c denotes the shear strength and flexural strength of the link-to-beam connection, e' denotes the end-to-end distance of shear link (see Figures 6 and 7), V_n denotes the nominal inelastic strength of shear link, and Ω denotes the link overstregnth factor.

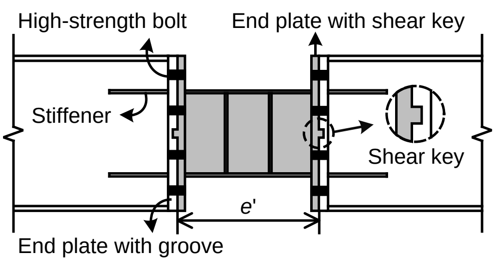

(a) Schematic drawing

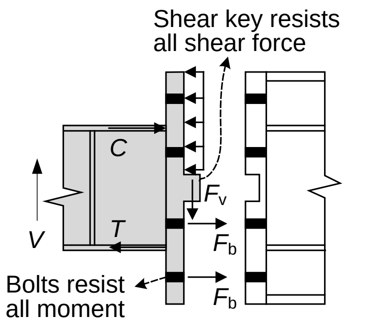

(b) Free body diagram for strength calculation

Figure 6. Link-to-beam end plate connection (with shear key)

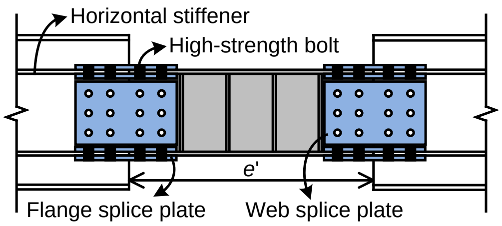

(a) Schematic drawing

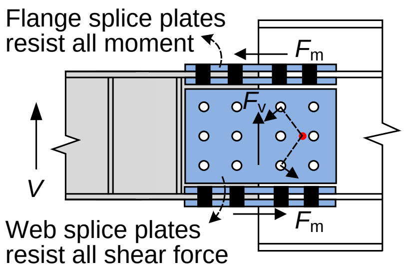

(b) Free body diagram for strength calculation

Figure 7. Link-to-beam splice plate connection.

As shown in Figure 6, the link end plate is connected to the end plate of the beam segment through a series of high strength bolts and shear key. Horizontal stiffeners are welded to the beam segments to be aligned with the flanges of the shear link. The end plates of the shear link are fabricated with a shear key, and those of the beam segments with a corresponding groove. The end plate connection is designed such that the shear key transfers all shear force and the high-strength bolts resist the bending moment. The presence of the shear key enables a significant reduction in the number of bolts required. The size of shear keys shall be determined to ensure their adequate shear strength and local compression-bearing strength capacity. The end plate thickness and high-strength bolt diameter are determined following a design procedure for end plate connections as set out in the AISC Design Guide Series 4 [21].

As shown in Figure 7, in the splice plate connection, the link web is spliced to the beam web in double shear. Horizontal stiffeners are welded to the beam segments to be aligned with the flanges of the shear link. The link flanges are also spliced to these horizontal stiffeners of the beam segments in double shear. High-strength bolts are used for the splice connections. The flange splices are designed to resist all the moment at the centerline of the splice, and the web splices are designed to resist all the shear force at the centerline of the splice. The required bolts for the web splice plate can be determined based on the eccentric shear strength calculated by the method of instantaneous center of rotation with the bolt load-deformation relationship developed by Kulak et al. [22].

Large-scale tests were conducted to examine the seismic behavior and replaceability of RSCBs adopting such link-to-beam connections. The hysteresis curves of the RSCBs with the end plate and splice plate connections are illustrated in Figures 8a and 9a, respectively. The end plate connection exhibits a stable hysteretic response with large inelastic deformations up to 0.06 rad. The splice plate connection developed inelastic rotations up to 0.08 rad. Bolt-slippage in the splice plate connections contributed to the coupling beam rotation and caused the noticeable "pinching" in the hysteresis response. Additional information on these test results can be found in Ji et al. [7].

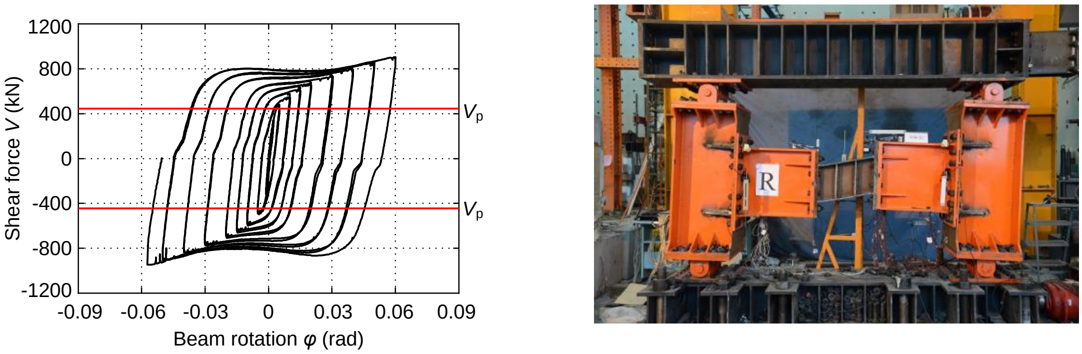

(a) Hysteretic response (b) Specimen at failure

Figure 8. Link-to-beam end plate connection behavior.

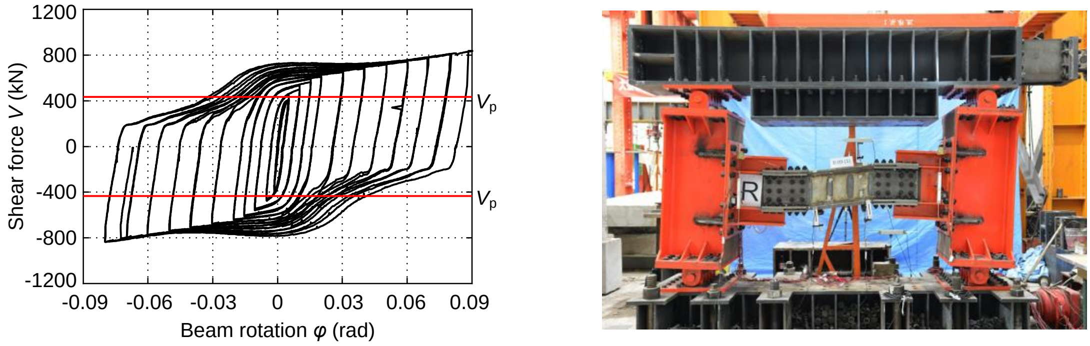

(a) Hysteretic response (b) Specimen at failure

Figure 9. Link-to-beam splice plate connection behavior.

An illustration of the failure mode states of RSCBs with the end plate connections and splice plate connections is shown in Figures 8b and 9b, respectively. The replacement of shear link was also conducted in these experiments. If the residual rotation of the coupling beam is no more than 0.0045 rad, both connection types enable easy replacement of the damaged links: the end plate connection was replaced in under 30 minutes and the splice place connection in 2.6 hours by two technicians. If the residual rotation of a coupling beam exceeds 0.0045 rad, drilling or welding may be required to enable the replacement of damaged links.

3.2. RC Slab above RSCB

The RC slabs above RSCBs are expected to experience large out-of-plane deformation and consequently suffer damage under large inelastic rotations. While the use of composite slabs above steel frame beams, where headed studs are used to achieve composite action, is common, large-scale tests of RSCBs with a composite slab illustrated that at a beam rotation of 0.04 rad, the composite slab suffered severe damage as a result of pulling out of shear studs and subsequent punching failure of the slab [23]. For ensuring minimal damage and easy post-earthquake repair of slabs, it is not recommended to use shear connectors between the RSCBs and RC slabs.

As opposed to engaging the slab in composite action with the beam, two alternatives are recommended: (i) bearing slab, and (ii) isolated slab. A schematic of these slab details is shown in Figures 10a and 11a. The bearing slab is cast above the RSCBs without shear connectors at the slab-beam interface. The isolated slab is elevated over the top flanges of the beam segments at a distance of over 0.03(*l*-*e*) to ensure that the RSCBs do not bear against the slab at an inelastic rotation of 0.06 rad, where *l* denotes the span of RSCB and *e* denotes the link length.

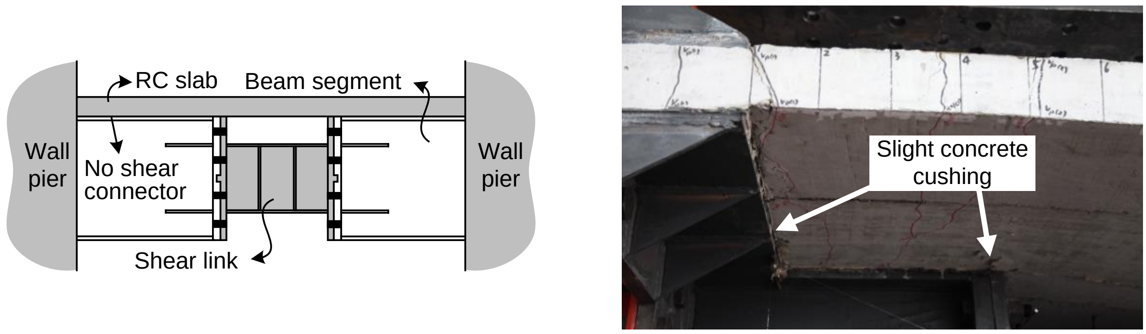

(a) Schematic (b) Damage at failure

Figure 10. Bearing slab.

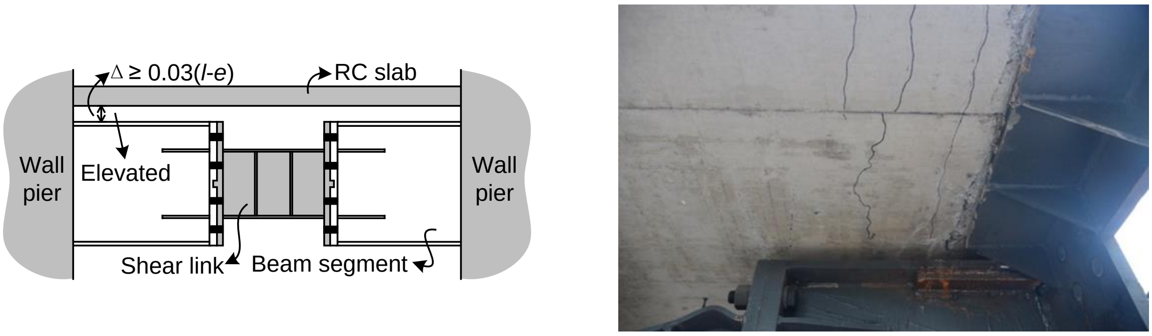

(a) Schematic (b) Damage at failure

Figure 11. Isolated slab.

Large-scale tests of the proposed connections illustrate cracks and slight concrete crushing on the bottom surface of the bearing slab in the region where the beam segments bore against the slab as seen in Figure 10b. The isolated slab developed much fewer and smaller cracks even a beam rotation of 0.05 rad, as shown in Figure 11b. The test results suggest that the RC slabs have limited effects on the shear strength and inelastic rotation capacity of the RSCBs. The bearing slab increases the initial elastic stiffness of the RSCBs by 36%, while the isolated slab does not provide additional elastic stiffness to the RSCBs. None of the slabs affect the loading and unloading stiffness of the RCSBs in the plastic stage of coupling beams. Therefore, in the modeling and design of RSCBs, the RC slab can be neglected due to its limited influence of shear strength, effective stiffness and inelastic rotation capacity of RSCBs.

3.3. Beam-to-wall Connection

The steel coupling beams are to be embedded into the RC wall piers by a sufficient distance to enable a complete transfer of the coupling forces through the interaction between the embedded steel beam and the surrounding concrete. The connection strength is developed from an internal moment arm by the bearing forces of concrete at two ends of the embedded steel beams (see Figure 12). AISC 341 [18] enables the calculation of the required embedment length to achieve the required strength of the beam-to-wall connection, as follows:

$$V_{\mathrm{e}} = 4.05\sqrt{f_c^{'}}\left(\frac{b_{\mathrm{w}}}{b_{\mathrm{f}}}\right)^{0.66}\beta_1 b_{\mathrm{f}} L_{\mathrm{e}}\left(\frac{0.58-0.22\beta_1}{0.88+g/\left(2L_e\right)}\right) \geq \Omega V_{\mathrm{n}} \tag{3}$$

where V_e denotes the strength capacity of beam-to-wall connection; f_c' denotes the concrete compressive strength, in MPa; b_w denotes the width of wall pier; b_f denotes the flange width of embedded beam; L_e denotes the embedded length of steel beam, which shall be considered to begin inside the first layer of confining reinforcement in the wall boundary element; β_1 is the factor relating depth of equivalent rectangular compressive stress block to depth of neural axis, as defined in ACI 318; $g=g_{clear}+2c$ denotes the effective span of RSCB, g_{clear} is the clear span of RSCB, and c is the thickness of the wall cover which is expected to suffer spalling at the wall face; V_n denotes the nominal inelastic strength of shear link; and Ω denotes the overstregnth factor of the shear link.

In order to ensure sufficient stiffness and ductility of the beam-to-wall connection detail, face bearing plates and transfer bars are required in the connections as shown in Figure 12. The detailing requirements can be found in AISC 341 [18]. Full-scale tests of the steel coupling beam-to-RC wall assembly were recently conducted by the authors for validation of the strength formulas and quantification of the joint damage at design force levels [24]. The test results indicate the damage to the joint is limited under the design force of steel coupling beams, with only slight cracks, which can be easily repaired with a surface finish (cosmetic repair).

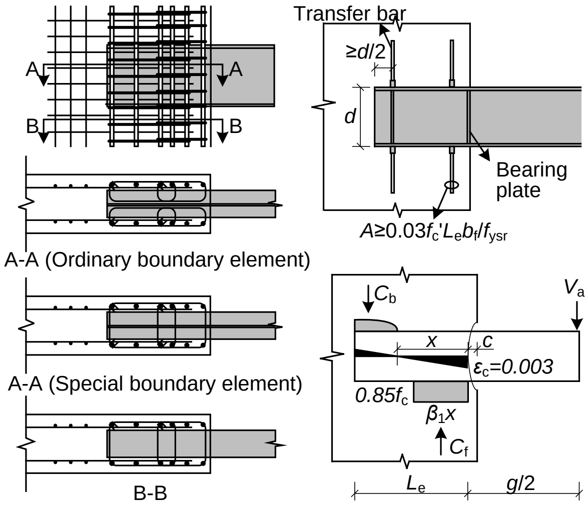

Figure 12. Steel beam-to-RC wall connection details and mechanism.

4. STRUCTURAL ANALYSIS MODELLING

4.1. Linear Elastic Analysis

The effective flexural stiffness of the tension and compression walls should be determined from a rational analysis method that includes a fiber section analysis, even if this requires iterations on the appropriate level of axial load to use in the analysis. Alternatively, recommendations for reduced section properties to account for cracking and loss of stiffness may be considered. For instance, according to US standards [1], the effective flexural stiffness of uncracked walls is $0.70EI_g$ and the effective flexural stiffness of cracked walls is $0.35EI_g$, where E is the modulus of elasticity and I_g is the gross moment of inertia of the concrete cross section. Similarly, according to Canadian standards [20], these values range from $0.50EI_g$ to $1.0EI_g$, with the exact value determined as a function of the response modification factor, system overstrength factor and moment load-to-capacity ratio of wall. The effective axial stiffness is $1.0EA_g$ for compression walls and 0.35 to $0.5EA_g$ for tension walls [2], where A_g is the gross cross-sectional area of the wall.

RSCBs should account for flexural and shear deformations in the beam segments and the shear link. This is essential because the shear deformations in such elements are not trivial. Additionally, the flexibility of the connection between the wall and the beam segments must be accounted for. The additional flexibility can be easily accounted for by implementing an effective fixed point at the end of beam segment that extends into the wall. Previous studies [2, 25] recommend this effective fixed point be taken at 30% of the embedment length from the face of the wall.

4.2. Non-linear Analysis Modelling

4.2.1 Wall Modelling

As structural walls would experience complicated nonlinear behavior, a multi-layer shell element is recommended for modeling the RC wall piers. The multi-layer shell element is developed based on the principles of composite material mechanics, and it is able to capture coupled in-plane and out-of-plane bending, and coupled in-plane bending and shear behavior of RC walls. In the multi-layer shell element, the concrete cover and inside concrete are represented by a number of concrete layers, and the distributed reinforcement is represented by the smeared rebar layers in the vertical and horizontal directions, respectively, as illustrated in Figure 13. Therefore, if the shear wall is subdivided into sufficient number of layers, the multi-layer shell element can reasonably simulate the actual stress distribution along the wall thickness. In the calculation, the strains and curvatures of the mid-layer are initially obtained, and then the strains in other layers are determined based on the plane-section assumption. Afterwards, the stresses of each integration point on each layer are calculated in accordance with the material constitutive law, and the internal forces of the element are calculated using the numerical integration method. Lu et al. [26] implemented the multi-layer shell element in the computation platform OpenSees [27] for modeling RC walls. Ji et al. [28] validated the models by comparison with test results and proved that the modeling approach could ensure both computational efficiency and a reasonable level of accuracy.

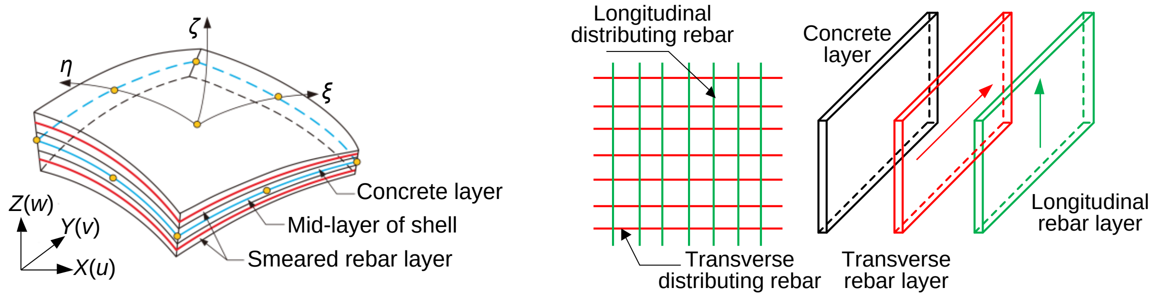

(a) Multi-layer shell element (b) Material layers

Figure 13. Sketch of multi-layer element for RC wall [26].

The concrete in structural walls is simulated as the planar concrete constitutive model, which is based on the damage mechanics and the smeared crack model [26]. This model can capture the concrete cracking and aggregate interlocking, by reasonably setting the tensile parameters and the factor of reduced shear modulus. Well-calibrated concrete models are recommended to represent the uniaxial stress-strain relationship of the concrete. The Kent-Park model [29] is suggested to represent the compressive uniaxial stress-strain relationship of the concrete cover, where the peak strain and spalling strain can be assumed to be 0.002 and 0.005, respectively, and the post-spalling strength was taken as zero. The stirrup-confined concrete can be represented by the Saatcioglu-Razvi model [30], which takes into account the increase of the strength and ductility of concrete due to the confinement effect. The residual compressive strength after ultimate strain can be taken to be 0.2 times the peak strength of the concrete. The tensile uniaxial stress-strain relationship of concrete can be represented by a bilinear curve which takes into account the tension softening. The tensile strength of concrete can be taken as 0.1 times the peak compressive strength, and the ultimate tensile strain is assumed to be 0.001. Figure 14a shows the hysteresis curve used to represent the cyclic behavior of the concrete. Allowing for computational efficiency and convergence, an origin-oriented linear curve can be used for the unloading path, while it might lead to slight pinching in the analysis results.

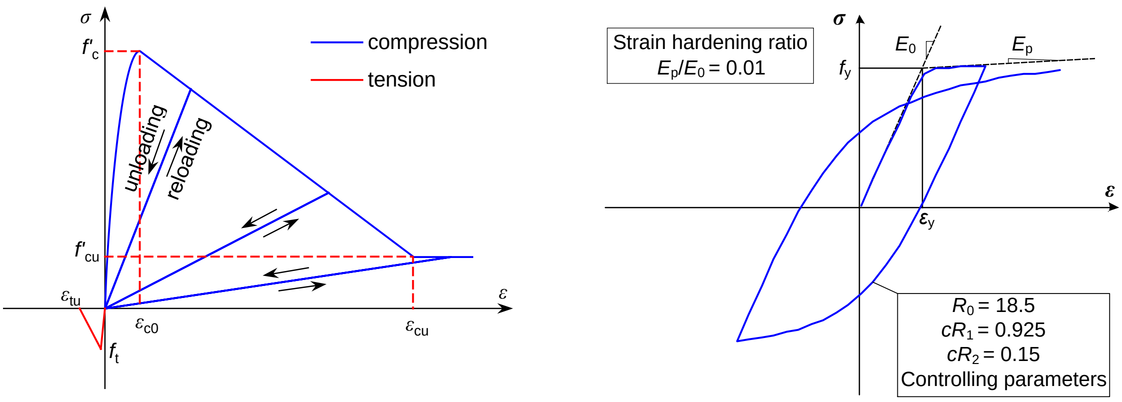

(a) Concrete (b) Steel

Figure 14. Hysteresis relationship curve for materials.

For steel reinforcement, the Menegotto-Pinto material model, known as Steel02 material in OpenSees [27] is recommended to represent the uniaxial stress-strain relationship, including the post-yield strain hardening and Bauschinger effect under cyclic loading. Figure 14b shows the cyclic stress-strain relationship curve for steel. The strain-hardening ratio, which denotes the ratio of post-yielding stiffness to the initial stiffness, can be taken as 0.01. The parameters R_0, cR_1 and cR_2, which control the curve shape of the transition from elastic to plastic branches, should be taken as 18.5, 0.925 and 0.15, respectively, in accordance with the recommendations by Taucer et al. [31].

4.2.2 RSCB Modelling

The RSCB model consists of three key components: shear link, beam segments and connections between them. Figure 15 shows the simplified numerical model for the RSCB.

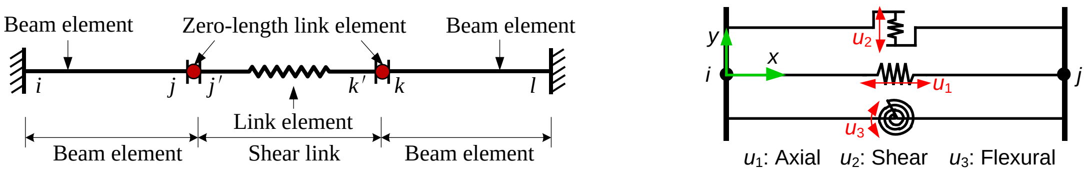

(a) Coupling beam model (b) Link element

Figure 15. Nonlinear model for RSCB [32].

The shear link is simulated by a nonlinear link element. The mechanical behavior on each degree of freedom can be modeled by a user-defined spring. For the shear link that has a length ratio less than 1.6 and is designed to yield in shear, the axial spring and flexural spring can be elastic, while the shear spring is nonlinear. Stiffness of the axial spring ($K_a=EA/e$) and stiffness of the flexural spring ($K_f=EI/e$) are calculated from the geometry of shear link and Young's modulus of the steel.

For the shear spring, the yield force V_y and shear stiffness K_s are calculated as follows:

$$V_{\mathrm{y}} = 0.6 f_{\mathrm{y,w}} A_{\mathrm{w}} \tag{4}$$

$$K_{\mathrm{s}} = \frac{1}{e^3/(12EI) + e/(GA_{\mathrm{w}})} \tag{5}$$

where $f_{y,w}$ denotes the yield strength of web steel, A_w denotes the cross-sectional area of the web, G denotes shear module of the web steel, E denotes Young modulus of the steel, I

denotes moment of inertia of the section and e denotes length of the shear link. Experiments by Ji et al. [9] report that shear links present similar hysteretic performance with the steel under cyclic loading. Thereby hysteretic behavior of the nonlinear shear spring is characterized by OpenSees uniaxial material model Steel02, which is based on Giuffré-Menegotto-Pinto hysteretic model [28]. The parameters of the hysteretic model are determined with trail and error procedure by calibrations against experiment data. The parameters R_0, cR_1 and cR_2 that reflect the Bauschinger effect are suggested to be taken as 18.5, 0.9 and 0.1 respectively. The parameter b that represents kinematic hardening effect is recommended to be takes as 0.003, and the parameters a1 through a4 that represent isotropic hardening effect are suggested to be taken as 0.14 (for a1 and a3) and 1.0 (for a2 and a4).

The beam segment is designed to remain elastic under seismic action, and thereby it can be modeled by elastic beam elements. Because the span-to-depth ratio of the beam segment is relative small and shear deformation is not negligible, the Timoshenko beam elements are required. A zero-length link element might be set between the beam segment element and the shear link element as shown in Figure 15, which is used to represent the local deformation of the link-to-beam connection if necessary.

5. APPLICATION OF NOVEL HCW SYSTEM AND PERFORMANCE IMPACTS

To date, a few high-rise buildings have been constructed using the HCW system with RSCBs. One of the pioneered applications of this novel system is the Sancai Building in Beijing, as shown in Figure 16. This 11-story building adopts a RC frame-shear wall interacting system. The total height of the structure is 48.5 m, and the plan dimension is 48.6 m by 17.65 m. Figure 17 shows a representative floor plan of the building. This building is designed per modern Chinese standards [33, 34]. The first author was engaged in the design of RSCBs and coupled walls in this building. The coupling ratio of the coupled walls in this buildings is approximately 0.45. The design of shear links, link-to-beam connections, beam segment, beam-to-RC wall connection, and isolated floor slabs is in accordance with the considerations described previously. A detailed description of the design process and resulting member sizes and details can be found in [32] and [35].

Using this project as a case study, Ji et al. [32] benchmarked the expected seismic performance of a characteristic coupled wall elevation within the building adopting the a HCW with RSCBs, against an equivalent design using conventional RC coupling beams. The responses of both systems are evaluated through nonlinear response history analysis. Four earthquake ground motion shaking intensities with distinct probabilities of exceedance (PoE) are considered, including SLE or service level earthquake (PoE: 63% in 50 years), DBE or design basis earthquake (PoE: 10% in 50 years), MCE or maximum considered earthquake (PoE: 2% in 50 years), and VRE or very rare earthquake (PoE: 0.5% in 50 years).

Figure 16. Illustration of Sancai Building adopting a HCW system with RSCBs.

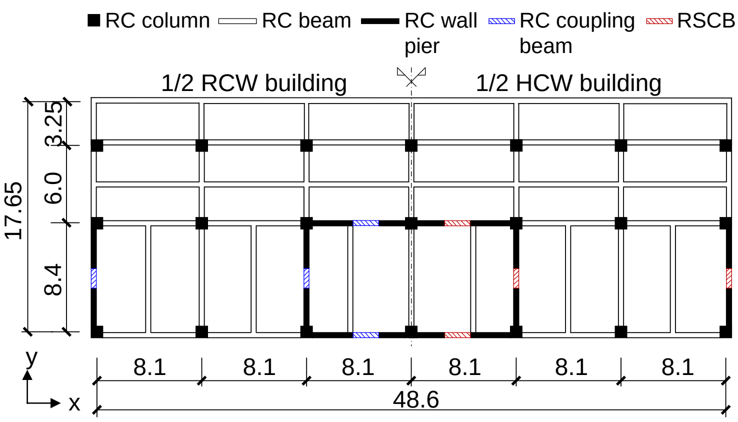

Figure 17. Plan view of prototype structure (Units in meter).

This study finds that under SLE shaking, the HCW and RCW systems produce consistent results. However, under DBE, MCE and VRE, the maximum interstory drift ratios of the HCW are 16%, 29% and 31% smaller than those of RCW, respectively. The reduction in peak drifts is attributed to the stable hysteretic response with large energy dissipation and overstrength of the RSCBs versus the limited overstrength and significant stiffness degradation of the RC coupling beams. Similar observations are reported when comparing the peak beam rotations with identical results under SLE and peak rotations 24%, 36% and 42% smaller in the RSCBs than those of the RC coupling beams, under DBE, MCE and VRE, respectively.

Regarding shear demands in the coupling beams, at SLE all coupling beams remain within the linear elastic range, at DBE all coupling beams yield with slight overstrength observed in the RC coupling beams, and considerable overstrength in the RSCBs. At MCE and VRE shaking, the RSCBs show significantly greater overstrength than the RC coupling beams. The variation in shear demands between RC coupling beams and RSCBs have a direct effect on the wall pier demands. Shear demands in the walls are well below their shear strength in both systems. However, there are more significant variations in the moment-axial demands between the RCW and HCW systems. The expected range of axial forces in the wall piers of an HCW system are expected to be greater than those of an RCW system due to the inherent overstrength of the RSCBs, which can lead to greater tensile and compressive forces in the wall piers. On the other hand, wall piers in an RCW system are expected to carry increased bending moments due to the stiffness degradation of RC coupling beams, which results in reduced coupling action and increased bending moments in the wall piers.

To further evaluate the implementation of a HCW system with RSCBs versus more conventional systems, fragility data for the RSCBs is required. To permit such studies, Ji et al. ([23], [35]) proposed fragility and consequence data for these innovative structural components, as this data is not available within the fragility database of the FEMA P-58 project. The recommended fragility and consequence data is summarized in Table 1.

Table 1. RSCB fragility and consequence function data ([23, 35]).

Damage state	Damage description	Repair method	Fragility data	Consequence function data		
				Quantity	Repair Cost ($)	Repair time (day)
DS1	RC slab damage	Epoxy injection or replacement of local slab	Median: 5% Dispersion: 0.30	Min: 2 Max: 5	Min: 16712 Max: 25068 β: 0.31	Min: 10.00 Max: 15.00 β: 0.40
DS2	Link web or flange buckling	Heating or replacing shear link	Median: 9% Dispersion: 0.19	Min: 2 Max: 5	Min: 18357 Max: 27535 β: 0.27	Min: 11.04 Max: 16.55 β: 0.37
DS3	Link facture	Replacement of shear link	Median: 11% Dispersion: 0.15	Min: 2 Max: 5	Min: 18357 Max: 27535 β: 0.27	Min: 11.04 Max: 16.55 β: 0.37

Notes: RSCBs' EDP is shear link rotation. β denotes dispersion.

In terms of damage to structural components, Ji et al. [32] find that damage to the RC wall piers is very limited in both the HCW and the RCW, even under VRE events, with expected damage only requiring surface finish repairs. Overall, expected damage is very low because of the high structural stiffness required by Chinese codes. At high intensities of ground shaking, moderate to severe damage is expected in the RC coupling beams, leading to cracks, spalling and crushing of concrete, buckling and fracture of reinforcement. However, the RSCBs sustain damage to the slab above the beam and possible web buckling of shear links. The study highlights the benefits of the HCW with RSCBs over the RCW system, because of easy replacement of the shear links as opposed to costly and time-consuming repairs of RC coupling beams.

In order to characterize performance beyond the response of the structural system under consideration, Ji et al. [35] extend their initial evaluation to consider the impact of adopting a HCW system with RSCBs versus a RCW system with RC coupling beams at building level. The study considers the performance of structural elements other than the coupled shear walls, as well as non-structural building components that are susceptible to seismic damage. The quantities and distribution of vulnerable structural components is estimated using the FEMA P-58 Normative Quantity Estimation Tool for an office building and the probabilistic performance calculations are carried out in SP3 [36], which implements the FEMA P-58 method [12].

In terms of engineering demand parameters, the maximum interstory drift ratio of the HCW building is up to 24.5% smaller at MCE and 32.7% smaller at VRE than the RCW building (consistent with the results of the initial study for a single wall elevation). The floor accelerations of both HCW and RCW buildings are of similar magnitude, indicating that use of HCWs is likely to have limited influence on suppressing floor accelerations. The results, expressed in terms of repair cost and repair time, indicate that at high intensities of ground shaking, namely MCE and VRE, most of the damage is concentrated in the coupling beams and nonstructural components. The resulting expected repair cost of the HCW building is 50.8% lower at MCE and 41.9% lower at VRE than that of the RCW building. Due to the easy replacement of damaged shear links in RSCBs, the HCW building also shows enhanced performance with regards to reductions in repair time. The expected time of repairs in series for the HCW building is 60.5% lower at MCE and 50.4% lower at VRE than that of the RCW building.

The performance assessment of the Sancai Building clearly demonstrates the impact of adopting a HCW system with RSCBs as opposed to an RCW system with RC coupling beams. It is indicated that through a small number of modifications of design, which have little impact on the design process, the widely adopted coupled wall structural system can be significantly improved to provide designs of greater seismic performance and resilience of high-rise buildings. Besides, the construction experience of the Sancai Building implies that construction cost of RSCBs is slightly higher than that of RC coupling beams, and the construction speed of the HCWs is comparable as the conventional RCWs.

6. APPLICATION OF RSCBS IN SUPER-TALL BUILDINGS IN CHINA

Except for common high-rise buildings, the RSCBs can be also used in the core walls of the super-tall buildings. As there are a large number of coupling beams in a super-tall buildings, it is no necessary to adopt RSCBs in all locations, considering that the RSCBs usually provides smaller stiffness than RC coupling beams. A reasonable solution is to assign RSCBs at the locations where the shear displacement demanding is very significant, while RC coupling beams remain in other locations. When subjected to strong ground motions, the RSCBs would undergo inelastic deformation and dissipate seismic energy through the yielding of 'fuse' shear links.

With this concept, RSCBs have been used in a few super-tall buildings in China. Among them, the Tianjin Goldin 117 Tower might be the first application of RSCBs in super-tall buildings. The building includes a total of 117 stories, with a height of 597 m. The plan dimension is 65 m by 65 m at the ground level, and it gradually reduced to 45 m by 45 m at the roof level. The building uses a mega braced frame-core wall system. The first three natural periods of the building is 9.06, 8.97 and 3.46 s, corresponding to the vibration modes of translation in two particular directions and the torsional mode, respectively [37]. The building site corresponds to the seismic fortification intensity of 7, with the peak ground acceleration of 0.15g for the DBE. The RSCBs are adopted in a few middle stories of core walls where the shear demanding is large. The shear links are made of Q235 steel (nominal yield strength f_y = 235 MPa), and their plastic shear strength is approximately 1000 kN. The beam segments are made of Q345 steel (f_y = 345 MPa). The middle 'fuse' shear link is connected to the beam segments through the end plate connections with shear keys, as shown in Figure 18. The beam segments and link-to-beam connections are capacity designed, ensuring that they remain elastic after the yielding and hardening of shear link. Note that steel reinforced concrete (SRC) walls, which consists of structural steel embedded in the boundary elements, are used in this super-tall building for enhancing seismic performance. Therefore, the RSCBs are rigidly jointed to the embedded steel column using complete-joint-penetration (CJP) groove welds. The design of SRC wall-steel beam connection is beyond the scope of this paper, and the design formulas and associated details can be found in Li et al. [38].

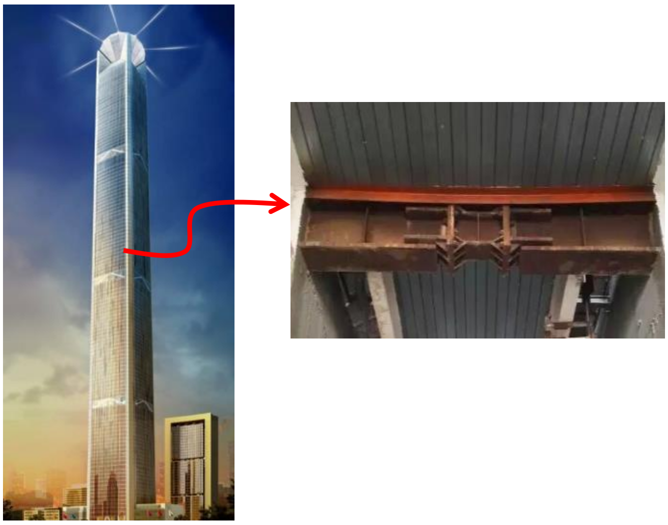

Figure 18. Illustration of Tianjin Goldin 117 Tower adopting RSCBs.

Another super-tall building that adopts the RSCBs is the China Zun Tower (also named Beijing Z15 Tower), which is located in the Beijing center business district. This building has a total of 108 stories with a height of 528 m. The plan dimension is 78 m by 78 m at the ground level. The mega braced frame-core wall system is adopted in this building. The first three natural periods are 7.90, 7.87 and 3.40 s, corresponding to the vibration modes in two translational directions and the torsional mode, respectively [39]. The site corresponds to the seismic fortification intensity of 8, with the peak ground acceleration of 0.2g for the DBE. The coupling beams in core wall are identified as the major energy-dissipating components when subjected to severe ground motions. It is notable that the double coupling beams, instead of one deep coupling beam, are used for improving the ductility and easily passing through the pipelines. A total of 160 RSCBs are designed and installed at the 59-72, 75-86, and 89-102 floors, as the lower beams of the double coupling beam system. The lower RSCB is designed to yield ahead of yielding of the above RC coupling beam. To ensuring the initial yielding of RSCB at a very small displacement of 1.5 mm, a very short shear link is assigned in the mid-span of RSCB, as shown in Figure 19. The shear links are made of the Q235 steel, while the beam segments of Q345 steel. The designed yield shear strength of the shear link is 350 kN. The end plate connection with shear key is used to joint the link to the beam segment, and the beam segments are rigidly jointed to the SRC wall piers.

Figure 19. Illustration of China Zun Tower (Beijing Z15 Tower) adopting RSCBs.

7. CONCLUSIONS

This paper provides an overview of seismic design considerations of an innovative structural system: HCW with RSCBs. Design procedure and detailed recommendations for a number of key design issues are provided to enable the adoption of this system by practicing engineers. From a case study of a high-rise building that adopts this system, the benefit of using this system for enhancement to overall building performance is highlighted. The results suggest that through a small number of modifications, which have little impact on the design process, the widely adopted coupled wall structural system can be significantly improved to provide designs of greater seismic resilience. In the end, this paper presents a few real-world applications of RSCBs in super-tall buildings in China.

ACKNOWLEDGMENTS

The work presented in this paper was sponsored by the National Key R&D Program of China (Grand No. 2018YFC1504401), Beijing Natural Science Foundation (Grant No. JQ18029) and National Natural Science Foundation of China (Grant No. 51678347). The authors wish to express their sincere gratitude to the sponsor. The authors also would like to thank Dr. Jie Jing (structural designer of Sancai Building), Mr. Jianlong Zhou and Mr. Lianjin Bao (structural designers of Tianjin Goldin Tower) and Mr. Wuhui Qi and Mr. Weibiao Yang (structural designers of China Zun Tower) for discussion and providing documents.

REFERENCES

[1] American Concrete Institute (ACI). Building code requirements for structural concrete (ACI 318M-14) and commentary (ACI 318RM-14). Farmington Hills, MI: ACI; 2015.

[2] El-Tawil S, Harries KA, Fortney PJ, Shahrooz BM, Kurama Y. Seismic design of hybrid coupled wall systems: state of the art. J Struct Eng 2010; 136(7): 755-69.

[3] El-Tawil S, Fortney PJ, Harries KA, Hassan M, Kurama Y, Shahrooz BM, Tong X. Recommendations for seismic design of hybrid coupled wall systems. Reston, VA: American Society of Civil Engineers; 2010.

[4] Fortney PJ, Shahrooz BM, Rassati GA. Large-scale testing of a replaceable "Fuse" steel coupling beam. J Struct Eng 2007; 133(12): 1801-7.

[5] Montgomery M, Christopoulos C. Experimental validation of viscoelastic coupling dampers for enhanced dynamic performance of high-rise buildings. J Struct Eng 2015; 141(5): 04014145.

[6] Lu X, Chen C, Chen Y, Shan J. Application of replaceable coupling beams to RC structures. Struct Des Tall Special Build. 2016; 25(17): 947-966.
[7] Ji X, Wang Y, Ma Q, Okazaki T. Cyclic behavior of replaceable steel coupling beams. J Struct Eng 2017; 143(2): 04016169.
[8] Lu X, Chen C, Jiang H, Wang S. Shaking table tests and numerical analyses of an RC coupled wall structure with replaceable coupling beams. Earthquake Engng Struct Dyn, 2018, 47(9): 1882-1904.
[9] Ji X, Wang Y, Ma Q, Okazaki T. Cyclic behavior of very short steel shear links. J Struct Eng 2016; 142(2): 04015114.
[10] Okazaki T, Arce G, Ryu HC, Engelhardt MD. Experimental study of local buckling, overstrength, and fracture of links in eccentrically braced frames. J Struct Eng 2005; 131(10): 1526-1535.
[11] American Society of Civil Engineers (ASCE). Minimum design loads and associated criteria for buildings and other structures (ASCE/SEI 7-16). Reston, VA: ASCE; 2017.
[12] Federal Emergency management agency (FEMA). Seismic performance assessment of buildings (FEMA P-58). Redwood City, CA: FEMA, 2012.
[13] Ministry of Housing and Urban-Rural Development of China (MOHURD). Chinese technical guideline of peer review for seismic design of super-tall buildings. Beijing: MOHURD; 2015 (in Chinese).
[14] Ji X, Cheng X, Xu M. Coupled axial tension-shear behavior of reinforced concrete walls. Eng Struct; 167: 132-42.
[15] Harries KA. Ductility and deformability of coupling beams in reinforced concrete coupled walls. Earthq Spectra 2001; 17(3): 457-78.
[16] El-Tawil S, Kuenzli CM, Hassan M. Pushover of hybrid coupled walls. I: design and modeling. J Struct Eng 2002; 128(10): 1272-81.
[17] Liu D. Study on seismic behavior and resiliency of novel hybrid coupled walls (master thesis). Beijing, China: Tsinghua University; 2017 (in Chinese).
[18] American Institute of Steel Construction (AISC). Seismic provisions for structural steel buildings (ANSI/AISC 341-10). Chicago, Il: AISC; 2010.
[19] Dusicka P, Itani AM, Buckle IG. Cyclic behavior of shear links of various grades of plate steel. J Struct Eng 2010; 136(4): 370-8.
[20] Canadian Standards Association (CSA). Design of concrete structures. Mississauga, Ontario: CSA; 2015.
[21] Murray TM, Summer EA. Extended end-plate moment connection□seismic and wind applications. Steel design guide series 4. 2nd ed. Chicago, Il: American Institute of Steel Construction (AISC); 2003.
[22] Kulak GL, Fisher JW, Struik JHA. Guide to design criteria for bolted and riveted joints. 2nd ed. New York: Wiley; 1987.
[23] Ji X, Wang Y, Zhang J, Okazaki T. Seismic behavior and fragility curves of replaceable steel coupling beams with slabs. Eng Struct 2017; 150: 622-35.
[24] Liang T. Study on seismic behavior and design of connections between steel coupling beams and wall piers (master thesis). Beijing, China: Tsinghua University; 2017 (in Chinese).
[25] Gong B, Shahrooz BM, Gillum AJ. Cyclic response of composite coupling beams. ACI special publications 1998; 174: 89-112.
[26] Lu X, Xie L, Guan H, Huang Y, Lu X. A shear wall element for nonlinear seismic analysis of super-tall buildings using OpenSees. Finite Elem Anal Des 2015, 98:14-25.
[27] OpenSees, Open System for Earthquake Engineering Simulations, in, Pacific Earthquake Engineering Research Center, http://opensees.berkeley.edu/.
[28] Ji X, Sun Y, Qian J, Lu X. Seismic behavior and modeling of steel reinforced concrete (SRC) walls. Earthquake Eng Struct Dyn 2015, 44(6): 955-72.

[29] Kent DC, Park R. Flexural members with confined concrete. Journal of the Structural Division 1971; 97(7): 1969-90.
[30] Saatcioglu M, Razvi SR. Strength and ductility of confined concrete. J Struct Eng 1992; 118(6): 1590-1607.
[31] Taucer FF, Spacone E, Filippou FC. A fiber beam-column element for seismic response analysis of reinforced concrete structures. Report UCB/EERC-91/17. Berkeley, CA: Earthquake Engineering Research Center, University of California at Berkeley; 1991.
[32] Ji X, Liu D, Sun Y, Molina Hutt C. Seismic performance assessment of a hybrid coupled wall system with replaceable steel coupling beams versus traditional RC coupling beams. Earthquake Eng Struct Dyn 2017, 46(4): 517-535.
[33] Ministry of Housing and Urban-Rural Development of China (MOHURD). Code for seismic design of buildings (GB 50011-2010), Beijing, China: Architecture & Building Press; 2016.
[34] Ministry of Housing and Urban-Rural Development of China (MOHURD). Technical Specification for Concrete Structures of Tall Building (JGJ 3-2010). Beijing: China Ministry of Construction, 2010 (in Chinese).
[35] Ji X, Liu D, Molina Hutt C. Seismic performance evaluation of a high-rise building with novel hybrid coupled walls. Eng Struct 2018; 169: 216-25.
[36] SP3, Seismic Performance Prediction Program, in, https://www.hbrisk.com/.
[37] Liu P, Yin C, Lee K, Liu G, Huang X, Ho G, Lee A. Structural system design and study of Tianjin Goldin 117 mega tower. Building Struct 2012; 42(3): 1-9,19 (in Chinese).
[38] Ji X, Cheng Y, Leong T, Cui Y. Seismic behavior and strength capacity of steel coupling beam-SRC wall joints. Eng Struct 2019; 201: 109820.
[39] Li H, Qi W, Xu J, Gan M, Miao Q, Yang W, Chang W, Cong Z. Elastic-plastic time-history analysis in the construction drawing design phase of China Zun Tower. Building Struct 2015; 45(23): 9-14,58 (in Chinese).

AUTHORS' BIOGRAPHIES

Xiaodong Ji received his BE and PhD in Civil Engineering from Tsinghua University in 2002 and 2007. Prior to his appointment at Tsinghua University in 2009, he was a JSPS Postdoctoral Researcher at Kyoto University in Japan. Currently, he is an associate professor at Department of Civil Engineering, Tsinghua University. His research interests include development of high-performance structural components and systems for tall buildings, resilience-based seismic design of buildings, advanced dynamic testing methods in earthquake engineering.

Carlos Molina Hutt received his BSc in Civil Engineering from Villanova University in 2003, his MSc in Structural Engineering from Stanford University in 2009, and his PhD in Earthquake Engineering from University College London (UCL) in 2017. From 2009 to 2013, Carlos worked as a structural engineer for Arup in New York. He is currently Assistant Professor in the Civil Engineering Department at the University of British Columbia (UBC). He is a registered Professional Engineer (PE) in the State of California in the United States, and a Chartered Engineer (CEng) in the United Kingdom. His research interests include the seismic performance characterization of tall buildings, performance-based earthquake engineering and resilience-based design.